



HAL
open science

Athermal heterogeneous nucleation of freezing: numerical modelling for polygonal and polyhedral substrates

a L Greer, Stuart A. Reavley

► **To cite this version:**

a L Greer, Stuart A. Reavley. Athermal heterogeneous nucleation of freezing: numerical modelling for polygonal and polyhedral substrates. *Philosophical Magazine*, 2008, 88 (04), pp.561-579. 10.1080/14786430801898636 . hal-00513862

HAL Id: hal-00513862

<https://hal.science/hal-00513862>

Submitted on 1 Sep 2010

HAL is a multi-disciplinary open access archive for the deposit and dissemination of scientific research documents, whether they are published or not. The documents may come from teaching and research institutions in France or abroad, or from public or private research centers.

L'archive ouverte pluridisciplinaire **HAL**, est destinée au dépôt et à la diffusion de documents scientifiques de niveau recherche, publiés ou non, émanant des établissements d'enseignement et de recherche français ou étrangers, des laboratoires publics ou privés.



Athermal heterogeneous nucleation of freezing: numerical modelling for polygonal and polyhedral substrates

Journal:	<i>Philosophical Magazine & Philosophical Magazine Letters</i>
Manuscript ID:	TPHM-07-Nov-0317.R1
Journal Selection:	Philosophical Magazine
Date Submitted by the Author:	31-Dec-2007
Complete List of Authors:	Greer, A L; University of Cambridge, Department of Materials Science and Metallurgy Reavley, Stuart; University of Cambridge, Materials Science and Metallurgy
Keywords:	nucleation, solidification, supercooled liquids
Keywords (user supplied):	solid-liquid interface, heterogeneous nucleation



Athermal heterogeneous nucleation of freezing: numerical modelling for polygonal and polyhedral substrates

S. A. REAVLEY and A. L. GREER

University of Cambridge

Department of Materials Science & Metallurgy

Pembroke Street, Cambridge CB2 3QZ, UK.

In a number of cases of practical interest, nucleation of freezing occurs at small supercooling, on potent nucleant substrates. Nucleation is then deterministic, consisting of the onset of free growth at a supercooling related only to substrate size and shape. Existing analytical treatments have evaluated the critical supercooling only for substrates in the form of a plane circle or a sphere. We develop a numerical treatment for a substrate of arbitrary shape. Coefficients are derived to permit straightforward evaluation of the critical supercooling for shapes typical of actual nucleant particles.

Keywords: heterogeneous nucleation, nucleant substrate, solid-liquid interface, supercooling.

1. Introduction

In normal freezing, the nucleation of the crystalline phase occurs at small supercooling, and must be catalysed by heterogeneities. Nucleation is normally considered in terms of a steady-state rate at a given temperature, but, as first noted by Turnbull [1], this approach may be not appropriate in the presence of potent heterogeneous substrates. In that case, the number of nucleation events may be a time-independent function of the maximum supercooling reached. This is *athermal* nucleation, so-called because it does not involve thermal activation over an energy barrier. Rather, nucleation occurs when the critical nucleation radius, decreasing as the melt is cooled, sweeps past the size of pre-existing embryos on nucleant particles. Turnbull showed that nucleation of this type could explain the observed freezing kinetics of mercury droplets in an emulsion by postulating a size distribution of nucleant patches [1]; this size distribution could not be independently verified, however.

Athermal nucleation is of relevance in cases of practical interest where nucleation supercoolings are known to be small, such as the solidification of alloys [2] and the action of ice-nucleating agents in living systems [3, 4]. In the former case, the size distribution of nucleant particles has been measured and thus it has been possible to verify the model directly [2]. The most studied case is the grain refinement of aluminium alloys by inoculation with an Al-Ti-B addition. In that case nucleation is on the {0001} faces of particles of TiB₂ [5]. It is assumed that solid aluminium forms so easily on these

basal faces (by classical nucleation with a very small contact angle, or by adsorption) that this is not the barrier to grain nucleation. Rather the barrier is that for free growth from the particle, as shown in figure 1a. In this picture the hexagonal platelet particle is, for ease of analysis, taken to be a disc, with the solid nucleus forming on a circular face. The solid-liquid interface is in the form of a spherical cap. As the solid grows away from the planar face, the curvature of its interface with the melt must increase. This is possible only until the radius of curvature decreases to equal the critical radius r^* for nucleation at the given temperature, at which point growth must stop. Thus if the critical radius is greater than the particle radius R (i.e. $r^* > R$), free growth from the particle is not possible. The solid that has formed on the particle is a *dormant nucleus*, and can become a *transformation nucleus* (i.e. potentially leading to transformation of the whole melt) only when further cooling of the melt causes r^* to decrease until $r^* = R$. At this critical condition for the onset of free growth, the solid-liquid interface is in the form of a hemisphere, the most curved surface that can form bounded by the periphery of the circular face of the nucleant particle.

Figure 1 near here

For a simple substrate shape such as a plane circle, the onset of free growth can be treated analytically. The present work demonstrates a numerical treatment suitable for analysing nucleation from general substrate shapes. We consider nucleation not only from planar substrates but also from realistic three-dimensional particle shapes. In each case the numerical treatment yields a single coefficient relating the supercooling for the onset of free growth to a characteristic linear dimension of the substrate.

While the present treatment is for freezing, it must be noted that the same geometry can apply for other cases of nucleation. Notably, the nucleation of gas bubbles in a liquid, in particular from gas pockets in cavities of arbitrary shape, may be treated in a similar way. In the analysis of such cases, the supercooling (of interest as the driving force for solidification) must be replaced by supersaturation. Types of bubble nucleation have been classified by Jones et al. [6].

2. Free-growth model

We consider first the nature of nucleation on a plane circular substrate as illustrated in figure 1a. At a given supercooling, the work of formation W of the solid on the substrate can be calculated as a function of the height h of the spherical cap [7]. The condition $h = 0$ is taken to represent an infinitesimally thin planar coating of solid on the substrate, and W is set to zero at this point. At a supercooling, ΔT , less than that for the onset of free growth, ΔT_{fg} , the work shows a minimum and a maximum as h is increased. Figure 1b, adapted from [7], is plotted in terms of dimensionless quantities. The reduced work of formation W_r is defined by

$$W_r = W/W_{\Delta T_{fg}}^* , \quad (1)$$

where $W_{\Delta T_{fg}}^*$ is the critical work for homogenous nucleation at the free-growth supercooling ΔT_{fg} . The reduced height of the spherical cap is given by h/R , where R is the radius of the circular face of the nucleant particle. The minimum in the work represents the metastable condition of dormant solid on the nucleant particle. The evolution of this minimum (marked by dots in figure 1b) shows how the solid grows as the supercooling is increased. The maximum in the work (not shown in figure 1b, but visible in figure 4a) represents the unstable point for nucleation. Conventional nucleation could occur at a steady rate by thermal activation over the energy barrier given by the difference in energies between the minimum and maximum. As shown in earlier work, however, this barrier is so large for the known sizes of nucleant particles that thermal activation can be ignored [7]. Rather nucleation occurs as the supercooling is increased, as shown by the curves in figure 1b. The barrier decreases and goes to zero at the onset of free growth, $\Delta T/\Delta T_{fg}=1$.

The free-growth model has been applied successfully in analysing the grain refinement of aluminium alloys [2, 8]. With measured nucleant particle size distributions as input, it has been shown to predict quantitatively the variation of grain size with addition level of refiner, cooling rate, and solute content of the alloy. The different particle size distributions in refiners appear to be correlated with differing refining performance [9]. Furthermore, the predicted dependence of refiner performance on particle size distribution [10] has been used to develop refiners with improved performance [11]. The same basic model has been applied with success to the solidification of magnesium alloys [12, 13], and may work also for quite different systems such as ice nucleation in nature [4].

As shown in earlier work, the critical supercooling ΔT_{fg} for the onset of free growth from a planar circular substrate of radius R is given by

$$\Delta T_{fg} = \frac{2\sigma_{SL}}{\Delta s R} , \quad (2)$$

where σ_{SL} is the free energy per unit area of the solid-liquid interface, and Δs is the entropy of fusion per unit volume [2]. This relation is the only one used so far in free-growth modelling, despite the fact that real substrates are not plane circles. As noted above, nucleation on TiB_2 particles in Al-Ti-B grain refiners for aluminium appears to be on plane hexagonal faces. For Al-Ti-C refiners, in contrast, the nucleant substrates are particles of the cubic phase TiC; these have an octahedral habit [14], bounded by $\{111\}$.

For three-dimensional substrates, the onset of free growth has so far been analysed only for spheres [4]. In that case, the solid grows as a sphere coating the substrate, and its work of formation does not show a minimum as in figure 1b. Rather, the dormant nucleus before the onset of free growth must be only an infinitesimally thin coating on the substrate. (Given that nucleant substrates of practical interest are of

micrometre dimensions, the zero-thickness initial solid assumed in the modelling is a reasonable approximation to the thickness of real adsorbed layers, likely to be one or a few atomic monolayers.) The present work examines the nature of dormant nuclei on shapes, such as the octahedron, which are of practical relevance.

As noted above, the substrates of practical relevance are so large that thermal fluctuations are not significant at the onset of free growth. The solid-liquid interface can therefore always be taken to be in mechanical equilibrium, having a uniform total curvature. As described further in §3, there are numerical treatments for the calculation of such surfaces. We examine in particular the shape of the solid-liquid interface at the onset of free growth for a variety of substrate shapes. By calculating the shape for other conditions, the work of formation of the nucleus can be evaluated as a function of solid volume at any supercooling.

3. Methods

The free-growth model shows that substrate size is important. For generality, we take the characteristic linear dimension of any 2D or 3D substrate to be the radius R of the smallest sphere within which the substrate can be inscribed, i.e. the vertices defining the substrate shape must lie on the reference sphere. This is illustrated for the case of an octahedral substrate in figure 2.

Figure 2 near here

Surface Evolver is a public-domain finite-element package, developed by Brakke, and widely applied to problems involving the minimization of surface area [15–18]. A surface is represented by a triangular tessellation, which can be progressively refined to obtain the required accuracy. An initial surface, parameterized in terms of its vertex coordinates for a particular triangulation, is modified under volume and boundary constraints by iteratively moving vertices, and quickly converges to a local minimum in area. In the present work, *Surface Evolver* is used to find the minimal area A of the solid-liquid interface for a given solid volume V forming on a nucleant substrate. The solid is assumed always to wet the substrate perfectly, and thus it is not necessary to model the solid-substrate interface. Above the liquidus temperature, V is infinitesimally small and the solid-liquid interface conforms to the shape of the substrate. For 3-dimensional substrates, the co-ordinates x, y, z of vertices on the solid-liquid interface are subject to constraints. These are of the form

$$|x| + |y| + |z| \geq R_{\text{octahedron}} \quad (3)$$

for an octahedron, where R is the radius of the inscribing sphere (figure 2), and of the form

$$\sqrt{3}\max(|x|, |y|, |z|) \geq R_{cube} \quad (4)$$

for a cube. For planar substrates (circle, hexagon, square and equilateral triangle in the present work), an additional vertex is added below the surface, making the substrate shape an n -sided cone to satisfy the *Surface Evolver* requirement that bodies have an initial positive non-zero volume. In these cases, the vertices on the perimeter of the planar nucleant face are fixed, to prohibit solid contact with the sides of the cone. As for the three-dimensional case, interface vertices on the nucleant face are forbidden to penetrate the substrate.

In *Surface Evolver* a curved interface can be modelled arbitrarily closely by refining the triangular tessellation. Each refinement step quadruples the number of triangles, increasing the computation time and the possibility of accumulated numerical errors. An adequate degree of refinement was assessed from interface-area convergence as described by Bradley and Weaire [18].

The work of nucleation is given by

$$W = \sigma_{SL}A - \Delta s\Delta TV \quad , \quad (5)$$

taking the reference state ($V = 0$, $W = 0$) to be an infinitesimally thin coating of solid on the substrate. As in previous work [7], it is appropriate to present the results in dimensionless form. The reduced work W_r has already been defined (equation 1). The normalizing factor $W_{\Delta T_{fg}}^*$ is given by [7]:

$$W_{\Delta T_{fg}}^* = \frac{4\pi\sigma_{SL}R^2}{3} \quad . \quad (6)$$

We choose to represent the extent of growth of the solid not by its volume V , but by a linear dimension ρ , which is defined to be the radius of a sphere of volume V . This effective radius is normalized with respect to the characteristic substrate dimension R :

$$\rho_r = \rho/R \quad . \quad (7)$$

The dependence of W_r on ρ_r is calculated for particular values of the reduced supercooling given by

$$\Delta T_r = \Delta T/\Delta T_{fg} \quad . \quad (8)$$

In terms of these reduced quantities, equation (5) can be re-expressed as:

$$W_r = \frac{3A}{4\pi R^2} - 2\Delta T_r \rho_r^3 \quad , \quad (9)$$

showing that the dependence of W_r on ρ_r is independent of materials parameters. One hundred equally spaced values of ρ_r are taken over a range of ρ_r from 0 to as high as 3. For each ρ_r , the *Surface Evolver* finds the surface of invariant curvature that has minimum area. For each minimization 1000 iterations are used, ample to achieve convergence. In this way for each ρ_r , the reduced area A/R^2 and reduced work W_r are calculated.

4. Results

4.1. Planar substrates

The analytical free-growth modelling undertaken so far has been for substrates in the form of plane circles. The critical condition for free growth, i.e. the maximum-curvature surface, in that case is a hemisphere. The corresponding critical shapes for hexagonal, square and triangular substrates are shown in figures 3a-c. The hexagon is a good description of the {0001} face of a TiB_2 crystal, while the square and the equilateral triangle form a basis for the discussion of three-dimensional substrates (next section). Figure 3c shows most clearly that near any apex of a polygonal substrate, the solid-liquid interface can (indeed, must) have principal curvatures of opposite sign while maintaining an invariant total curvature.

Figure 3 near here

The dependence of W_r on ρ_r for each substrate shape is shown in figure 4 and compared with that for the plane circle. The dependence, plotted for reduced supercoolings ΔT_r of 0.5, 0.75, 1.0 and >1.0 , is similar in each case.

Figure 4 near here

When the liquid is supercooled, but before the onset of free growth, the work of formation of the nucleus as a function of its size shows a minimum and maximum. On further cooling these extrema converge, the onset of free growth is when the work of formation first decreases monotonically with nucleus size. For a plane circular substrate, the free-growth supercooling ΔT_{fg} is related to the substrate radius R by equation (2). This can be expressed in more general terms as

$$\Delta T_{fg} = \frac{2\beta\sigma_{LS}}{\Delta sR} \quad (10)$$

where β is a coefficient that takes the value 1 for a plane circle, but takes different values for differently shaped (planar or three-dimensional) substrates inscribed within a sphere of radius R . Values of β calculated in the present work are given in Table 1. The

standard error in these values is mainly from the error in area evaluation; this is due to *Surface Evolver*'s piecewise-linear approximation to a curved surface, and is evaluated by standard methods. The largest relative error, 2.2%, arises for the triangular substrate because of the high curvature of the solid-liquid interface near its corners.

For a given R , progressively greater supercooling is required (i.e. the β values increase) for the onset of free growth from a circle, a hexagon, a square and a triangle. This may be expected, since these shapes have progressively smaller areas (as can be judged from the outlines in figure 3). The areas of the polygons normalized with respect to the circle are given in Table 1. It is of interest to compare free-growth supercoolings for different substrate shapes of equal area, according to

$$\left(\frac{\Delta T_{fg}(\text{polygon})}{\Delta T_{fg}(\text{circle})} \right)_{\text{equal area}} = \beta(\text{polygon}) \left(\frac{A(\text{polygon})}{A(\text{circle})} \right)_{\text{equal } R}^{1/2}, \quad (11)$$

where $A(\text{polygon})$ and $A(\text{circle})$ are the areas of a polygon and a circle with equal inscribing radius R . The supercooling ratios for equal area are also given in Table 1. For shapes of equal area, the free-growth supercoolings for the polygons are only slightly greater than for the circle: 0.3% greater for the hexagon, 1.3% for the square and 4.8% for the equilateral triangle.

Table 1 near here

4.2. Three-dimensional substrates

The case of growth of a solid from a spherical substrate has already been treated [4]. In that case there is no metastable minimum in the work-of-formation curve; the critical shape for the onset of free growth is an adsorbed layer on the spherical substrate when the radius of the substrate equals the critical nucleation radius. We now examine more realistic three-dimensional substrate shapes. We note that nucleant substrate phases often have cubic crystal structures and that common habits of cubic-phase particles are octahedral (bounded by {111}) and cubic (bounded by {100}). Figure 5 shows the critical shapes for the onset of free growth from (a) octahedral and (b) cubic substrates. As for the planar substrates, it is clear that the solid-liquid interface near the apices of the substrate can have principal curvatures of opposite sign.

Figure 5 near here

Figure 6 near here

For solid forming on octahedral and cubic substrates the work of formation (figure 6b,c) does show a metastable minimum and an unstable maximum analogous to those for planar substrates (figure 4). For supercoolings less than ΔT_{fg} , the solid sits at

1
2
3
4
5
6
7
8
9
10
11
12
13
14
15
16
17
18
19
20
21
22
23
24
25
26
27
28
29
30
31
32
33
34
35
36
37
38
39
40
41
42
43
44
45
46
47
48
49
50
51
52
53
54
55
56
57
58
59
60

the metastable minimum and grows only as this minimum moves toward greater volume as the supercooling is increased. The sequence of shapes adopted by the solid during cooling is best appreciated from two-dimensional cross-sections. Figure 7 shows a sequence of these up to the critical condition from an octahedral substrate. Growth is most evident from the centres of the triangular faces. As the supercooling is increased, the solid-liquid interfaces on adjacent faces link at the mid-point of the edges and ultimately the solid-liquid interface stays in contact with the substrate only near the substrate apices. A similar sequence is evident for the growth from a cubic substrate (figure 8). For both these 3D substrates, the onset of free growth (figure 5) is reached just before the solid-liquid interface reaches the surface of the inscribing sphere, consistent with the values of β being somewhat greater than 1, as shown in Table 1.

Figure 7 near here

Figure 8 near here

5. Discussion

The values of β determined in the present work for simple polygonal and polyhedral substrates allow the critical supercooling for the onset of free growth to be calculated using equation (10). The present results also suggest how the effective size of a substrate can be estimated and show that in this respect 2D and 3D substrates must be considered separately. For 2D polygonal substrates with a given inscribing radius R , the critical supercooling increases significantly with decreasing number of sides. If substrates of equal area are compared, however, the critical supercooling increases only very slightly with decreasing number of sides. For 3D polyhedral substrates with a given R , the critical supercooling is only slightly greater than for the corresponding sphere. If a cube, an octahedron and a sphere of equal surface area were compared, the cube and octahedron would show critical supercoolings much less than that for the sphere.

These comparisons suggest that if the β value is not known for a given substrate shape, the critical supercooling can still be found to a reasonable approximation (at least when the substrate is equiaxed) by applying equation (2) directly. For 2D substrates, the value of R to use in equation (2) is that of a circle of *equal area*, while for 3D substrates it is not related to area but is the radius of the sphere within which they can be inscribed. In previous work analysing the inoculation of aluminium alloys [2], the hexagonal faces of TiB_2 particles were approximated as circular discs. This is now shown to be an excellent approximation if the hexagon is modelled as a circle of equal area.

For the cube and the octahedron considered in the present work, it is significant that dormant solid formed on the faces can link up (figures 5, 7, 8). In this way, the shape of the solid-liquid interface above a face of a polyhedral substrate can be quite different from the shape above a polygonal substrate with the same shape as the face. Using the β values in Table 1 we can compare the critical supercooling on a cubic substrate of given edge length with that on a square substrate with the same edge length.

1
2
3
4
5
6
7
8
9
10
11
12
13
14
15
16
17
18
19
20
21
22
23
24
25
26
27
28
29
30
31
32
33
34
35
36
37
38
39
40
41
42
43
44
45
46
47
48
49
50
51
52
53
54
55
56
57
58
59
60

It should be noted that in this comparison, the cubic substrate has a larger inscribing radius. The critical supercooling for the cube is 67% of that for the square, showing the significantly greater potency of the 3D shape. Making a similar comparison for an octahedron and an equilateral triangle of the same edge length, the effect is even stronger: The critical supercooling for the octahedron is 55% of that for the triangle.

The form of the work of nucleation as a function of solid growth also shows differences between 2D and 3D substrates. In the 2D case, the work always takes very similar forms (figure 4). When the liquid is supercooled but the condition for free growth has not yet been reached, the work always shows a metastable minimum and an unstable maximum. The minimum corresponds to a dormant solid nucleus on the substrate. In the 3D case, the depth of this minimum varies from shape to shape and it disappears totally for a spherical substrate (figure 6a), for which the dormant solid is just an infinitesimally thin coating.

The present results allow us to consider what shapes might be optimal for inoculant particles. The applicability of the free-growth model to heterogeneous nucleation of freezing depends on the nucleant substrate being “wetted” by the solid. In this way, the first formation of solid is not the rate-limiting factor for grain nucleation. Stabilized by adsorption effects, a solid coating on the substrate can exist even above the liquidus temperature [5]. Such a stabilization is weakened by convexity of the substrate surface because this forces the solid-liquid interface to be curved, and the Gibbs-Thomson effect then lowers the liquidus temperature. The convexity is greatest for spherical substrates. As noted above, the present work suggests that the effective size of an equiaxed 3D nucleant particle is well approximated by its inscribing sphere. But a particle with planar faces is preferable to the sphere because it avoids the problem of convexity. Indeed, it seems there would be benefits in having a 3D form with concave faces. Such a nucleant particle could combine stabilization of the solid phase on its surface with a large effective radius facilitating the onset of free growth of the solid. It would also tend to maximize the nucleation potency per volume of nucleant phase.

The present work is based on an isotropic solid-liquid interfacial energy. Even for simple systems, σ_{SL} is in fact mildly anisotropic, varying with orientation by up to a few percent [19]. Anisotropy is most likely to affect the work of formation of the nucleus in the early stages, when the solid-liquid interface is near-planar. At the critical condition for the onset of free growth, however, the solid-liquid interface approximates to a hemisphere or to a sphere, thus sampling all orientations, and largely averaging out any effects of anisotropy.

6. Conclusions

Heterogeneous nucleation of freezing at small supercoolings is athermal. It occurs on cooling and corresponds to the onset of free growth of the solid from the nucleant substrate at a supercooling inversely proportional to a linear dimension of the substrate. The free-growth model, previously applied analytically to substrates in the form of a

plane circle or a sphere, can be applied to substrates of arbitrary shape by using the *Surface Evolver* to treat the solid-liquid interface numerically, finding the minimum interfacial area for a given solid volume. The potency of different substrate shapes can be measured in terms of a coefficient β linking the free-growth supercooling to the radius R of the sphere within which the shape is inscribed. For plane circle and spherical substrates β has the value 1. The values of β have been calculated for 2D substrates (hexagon, square, equilateral triangle) and 3D substrates (octahedron, cube). For 2D substrates, as the polygon deviates more from the circle (i.e. has fewer sides), β increases (i.e. for a given R the critical supercooling is greater). For substrates of equal area, however, the supercooling necessary for the onset of free growth increases only slightly with deviation from the ideal circular shape. For example, the critical supercooling is just 4.8% greater for an equilateral triangle than for a circle of the same area. In contrast, for 3D substrates their surface area is not a good indicator of their potency. The coefficient β increases only slightly with deviation from sphericity, showing that 3D substrates have roughly the same potency as the sphere that encloses them. For example, the critical supercooling is just 3.9% greater for a cube than for its inscribing sphere. It is of interest to compare the nucleation potency of a planar polygonal substrate (e.g. a square) and a 3D substrate (the cube) with faces of the same shape and edge length as the polygon. The 3D substrate gives a much smaller critical supercooling, because the solid forming on it is not bounded by the face edges. All polygonal substrates show a similar form for the work of formation of solid as a function of a characteristic linear dimension. For supercoolings smaller than the critical value for free growth, the work shows a minimum and followed by a maximum. The minimum in the work defines a metastable condition of the dormant solid nucleus on the substrate. For polyhedral substrates, the depth of the minimum decreases as the polyhedron approximates more closely to a sphere and it disappears for spherical substrates. A nucleant particle should stabilize dormant solid before the onset of free growth and should have a large effective size to reduce the critical supercooling. The present results suggest that equiaxed particles with concave faces would be a desirable shape.

Acknowledgements

SAR is grateful to the Engineering and Physical Sciences Research Council for a studentship in support of this work.

References

- [1] D. Turnbull, *Acta Metall.* **1** 8 (1953).
- [2] A.L. Greer, A.M. Bunn, A. Tronche, *et al.*, *Acta Mater.* **48** 2823 (2000).
- [3] K.E. Zacharissen and H.T. Hammel, *Cryobiology*, **25** 143 (1988).

- 1
2
3 [4] A.L. Greer and T.E. Quested, *Phil. Mag.* **86** 3665 (2006).
4
5 [5] P. Schumacher, A.L. Greer, J. Worth, *et al.*, *Mater. Sci. Technol.* **14** 394 (1998).
6
7 [6] S.F. Jones, G.M. Evans and K.P. Galvin, *Adv. Coll. Inter. Sci.* **80** 27 (1999).
8
9 [7] T. E. Quested and A. L. Greer, *Acta Mater.* **53** 2683 (2005).
10
11 [8] Gilles Dour, *Aide-Mémoire Fonderie: Alliages, Procédés, Propriétés d'Usage, Défauts.* (Dunod, Paris 2004).
12
13 [9] W. Schneider, M.A. Kearns, M.J. McGarry, *et al.*, in *Light Metals 1998* (ed. B. Welch), pp. 953–961. (TMS, Warrendale, PA, 1998).
14
15 [10] T.E. Quested and A.L. Greer, *Acta Mater.* **52** 3859 (2004).
16
17 [11] Y.F. Han, D. Shu, J. Wang, *et al.*, *Mater. Sci. Eng.* **430** 326 (2006).
18
19 [12] R. Günther, Ch. Hartig and R. Bormann, *Acta Mater.* **54** 5591 (2006).
20
21 [13] M. Qian, *Acta Mater.* **55** 943 (2007).
22
23 [14] A. Tronche and A.L. Greer, *Phil. Mag. Lett.* **81** 321 (2001).
24
25 [15] K. Brakke, *Exp. Math.* **2** 141 (1992) (see also
26 www.susqu.edu/brakke/evolver/evolver.html).
27
28 [16] K. Brakke, *Phil. Trans. R. Soc. A* **354** 2143 (1996).
29
30 [17] K. Brakke and F. Morgan, *Eur. Phys. J. E* **9** 453 (2002).
31
32 [18] G. Bradley and D. Weaire, *Comput. Sci. Eng.* **6** 16 (2001).
33
34 [19] D.Y. Sun, M. Asta and J.J. Hoyt, *Phys. Rev. B* **69** 174103 (2004).
35
36
37
38
39
40
41
42
43
44
45
46
47
48
49
50
51
52
53
54
55
56
57
58
59
60

FIGURE AND TABLE CAPTIONS

Figure 1. Stages in the growth of solid from a circular nucleant substrate of radius R . (a) The solid-liquid interface takes the form of a spherical cap and in the critical condition for the onset of free growth it is a hemisphere. (b) The reduced work of formation of the solid W_r (equation 1) as a function of the reduced height h/R of the spherical cap for selected values of the reduced supercooling ΔT_r (equation 8) which is 1 at the onset of free growth.

Figure 2. An octahedral substrate inscribed within a sphere.

Figure 3. The shape of the solid-liquid interface, computed using *Surface Evolver*, at the critical condition for the onset of free growth from polygonal substrates: (a) hexagon, (b) square, and (c) equilateral triangle.

Figure 4. The reduced work of formation of the solid W_r (equation 1) as a function of a reduced linear dimension ρ_r (equation 7) for selected values of reduced supercooling ΔT_r (equation 8) for growth from planar substrates: (a) circle, (b) hexagon, (c) square, and (d) equilateral triangle.

Figure 5. The shape of the solid-liquid interface, computed using *Surface Evolver*, at the critical condition for the onset of free growth from polyhedral substrates: (a) octahedron, (b) cube.

Figure 6. The reduced work of formation of the solid W_r (equation 1) as a function of a reduced linear dimension ρ_r (equation 7) for selected values of reduced supercooling ΔT_r (equation 8) for growth from 3D substrates: (a) sphere, (b) octahedron, (c) cube.

Figure 7. Stages in the growth of the dormant solid nucleus on an octahedral substrate as the reduced supercooling ΔT_r is increased towards the critical value for the onset of free growth. At each stage, the solid-liquid interface is at a metastable position corresponding to the minimum in the work of formation shown on the curves in figure 6b. The shaded plane in (a) is that taken for the cross-sections in (b).

Figure 8. Stages in the growth of the dormant solid nucleus on a cubic substrate as the reduced supercooling ΔT_r is increased towards the critical value for the onset of free growth. At each stage, the solid-liquid interface is at a metastable position corresponding to the minimum in the work of formation shown on the curves in figure 6c. The two shaded planes in (a) are those taken for the cross-sections in respectively the left-hand and right-hand portions of (b).

Table 1. For polygonal and polyhedral substrates, the values of β (to which the critical supercooling for the onset of free growth is proportional) have been calculated using

1
2
3
4 *Surface Evolver.* For the 2D substrates, the relative areas for a given inscribing radius
5 and the relative critical supercoolings for a given area are also given.
6
7
8
9
10
11
12
13
14
15
16
17
18
19
20
21
22
23
24
25
26
27
28
29
30
31
32
33
34
35
36
37
38
39
40
41
42
43
44
45
46
47
48
49
50
51
52
53
54
55
56
57
58
59
60

For Peer Review Only

1
2
3
4
5
6
7
8
9
10
11
12
13
14
15
16
17
18
19
20
21
22
23
24
25
26
27
28
29
30
31
32
33
34
35
36
37
38
39
40
41
42
43
44
45
46
47
48
49
50
51
52
53
54
55
56
57
58
59
60

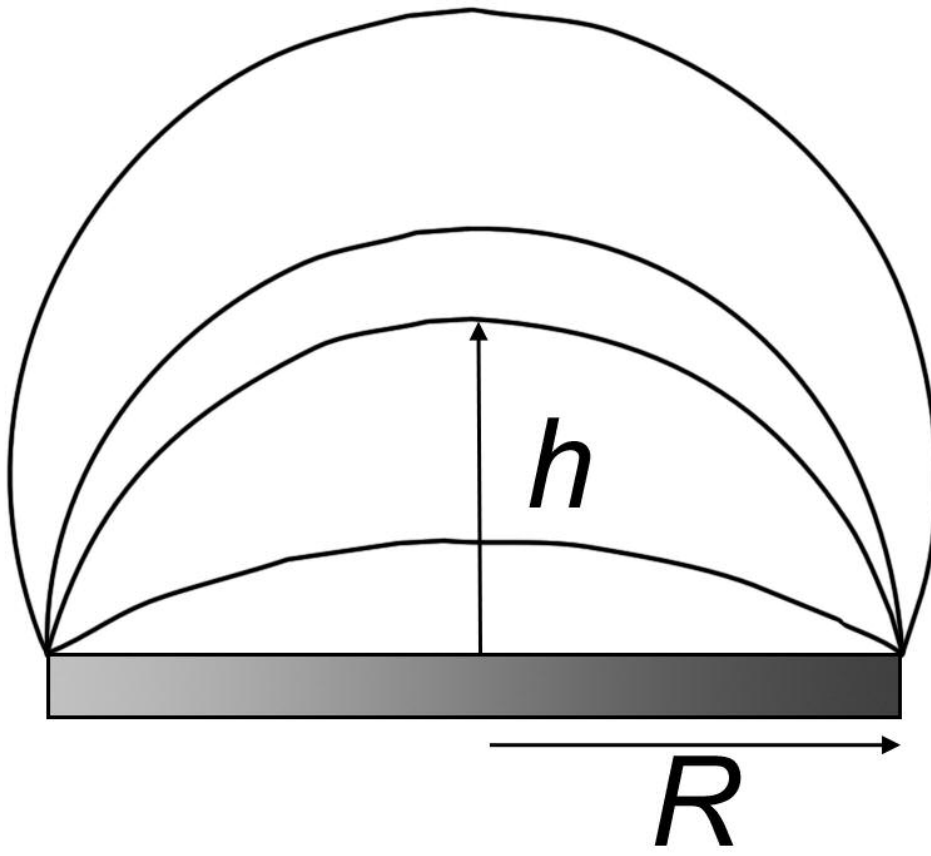


Figure 1a
282x282mm (72 x 72 DPI)

only

1
2
3
4
5
6
7
8
9
10
11
12
13
14
15
16
17
18
19
20
21
22
23
24
25
26
27
28
29
30
31
32
33
34
35
36
37
38
39
40
41
42
43
44
45
46
47
48
49
50
51
52
53
54
55
56
57
58
59
60

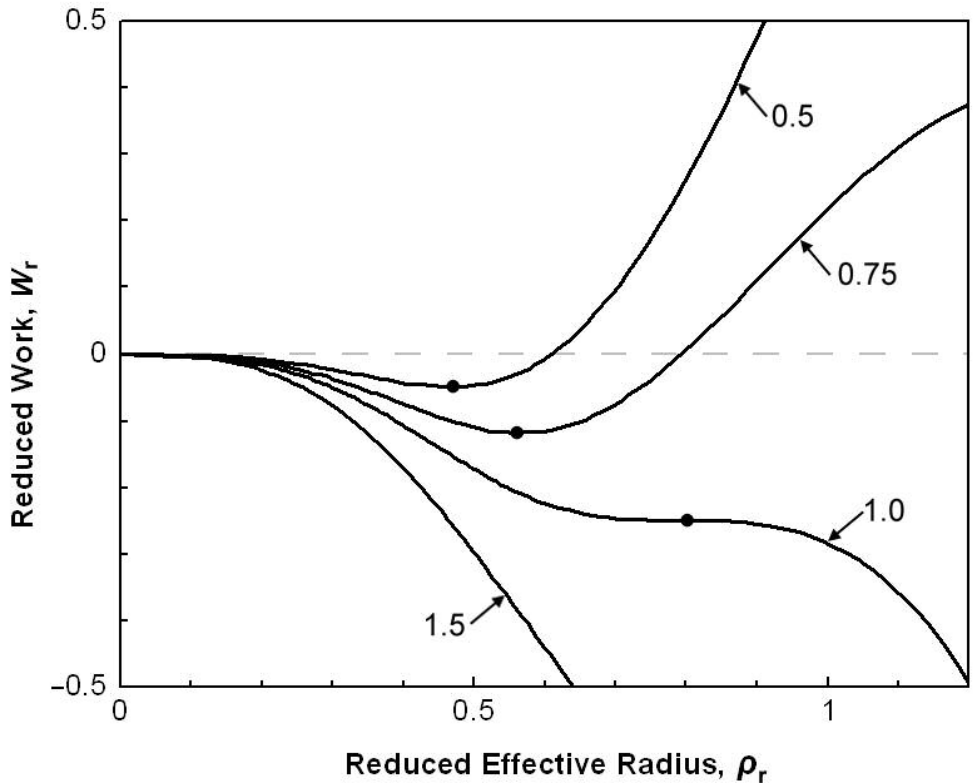


Figure 1b
282x225mm (72 x 72 DPI)

View Only

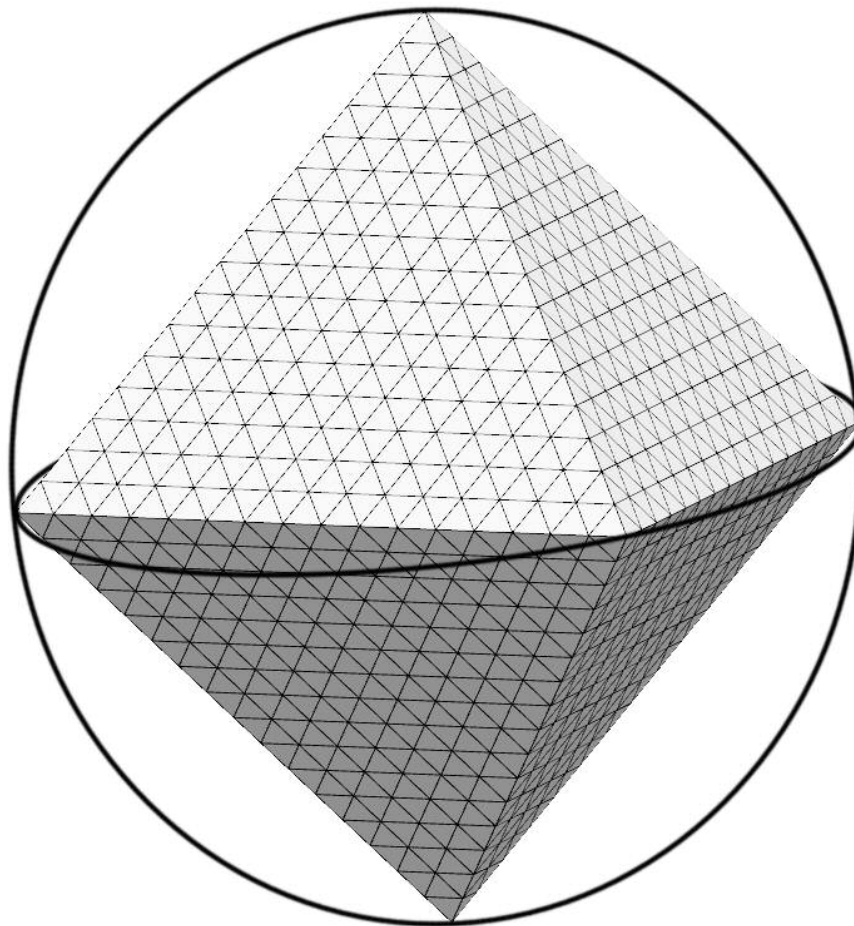


Figure 2
282x282mm (72 x 72 DPI)



1
2
3
4
5
6
7
8
9
10
11
12
13
14
15
16
17
18
19
20
21
22
23
24
25
26
27
28
29
30
31
32
33
34
35
36
37
38
39
40
41
42
43
44
45
46
47
48
49
50
51
52
53
54
55
56
57
58
59
60

1
2
3
4
5
6
7
8
9
10
11
12
13
14
15
16
17
18
19
20
21
22
23
24
25
26
27
28
29
30
31
32
33
34
35
36
37
38
39
40
41
42
43
44
45
46
47
48
49
50
51
52
53
54
55
56
57
58
59
60

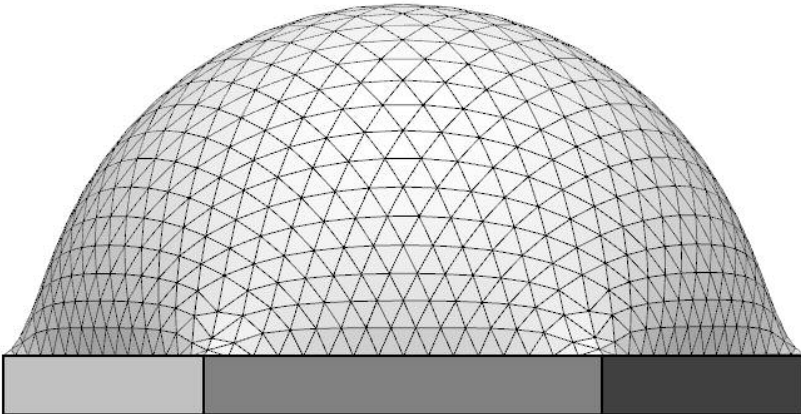


Figure 3a
282x282mm (72 x 72 DPI)



1
2
3
4
5
6
7
8
9
10
11
12
13
14
15
16
17
18
19
20
21
22
23
24
25
26
27
28
29
30
31
32
33
34
35
36
37
38
39
40
41
42
43
44
45
46
47
48
49
50
51
52
53
54
55
56
57
58
59
60

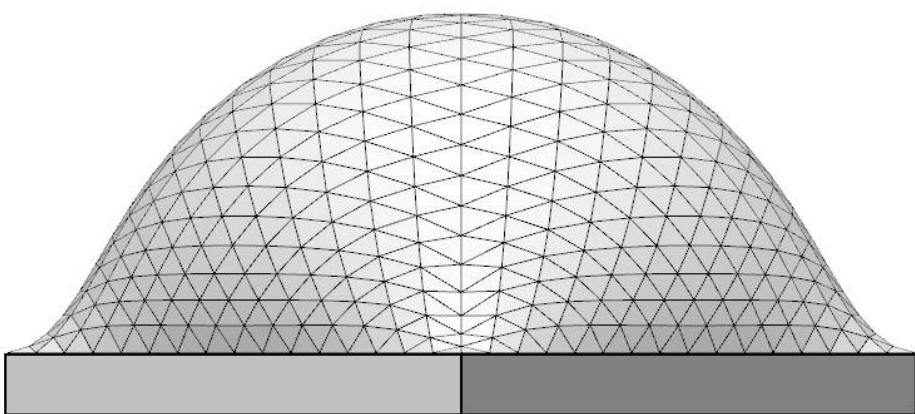


Figure 3b
282x282mm (72 x 72 DPI)



1
2
3
4
5
6
7
8
9
10
11
12
13
14
15
16
17
18
19
20
21
22
23
24
25
26
27
28
29
30
31
32
33
34
35
36
37
38
39
40
41
42
43
44
45
46
47
48
49
50
51
52
53
54
55
56
57
58
59
60

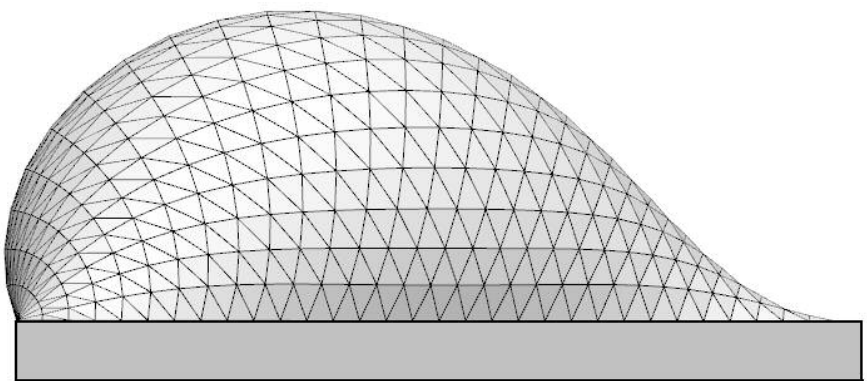
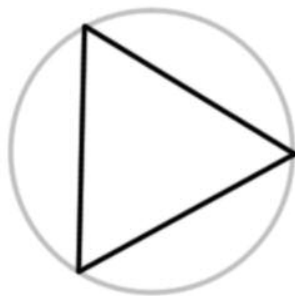


Figure 3c
282x282mm (72 x 72 DPI)



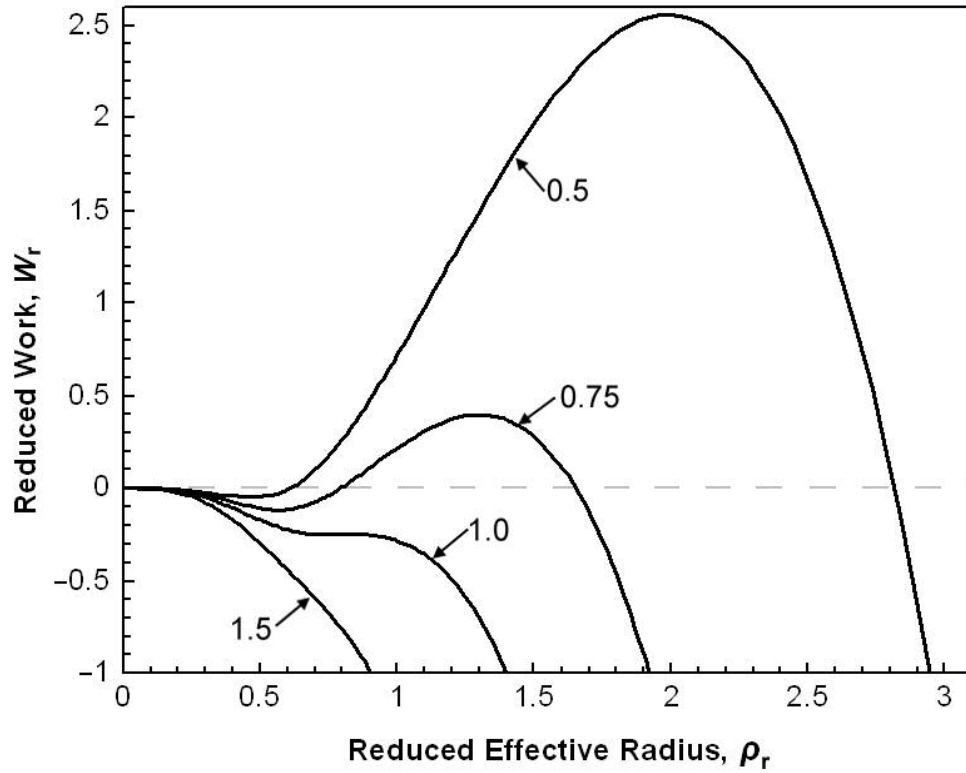


Figure 4a
282x225mm (72 x 72 DPI)

1
2
3
4
5
6
7
8
9
10
11
12
13
14
15
16
17
18
19
20
21
22
23
24
25
26
27
28
29
30
31
32
33
34
35
36
37
38
39
40
41
42
43
44
45
46
47
48
49
50
51
52
53
54
55
56
57
58
59
60

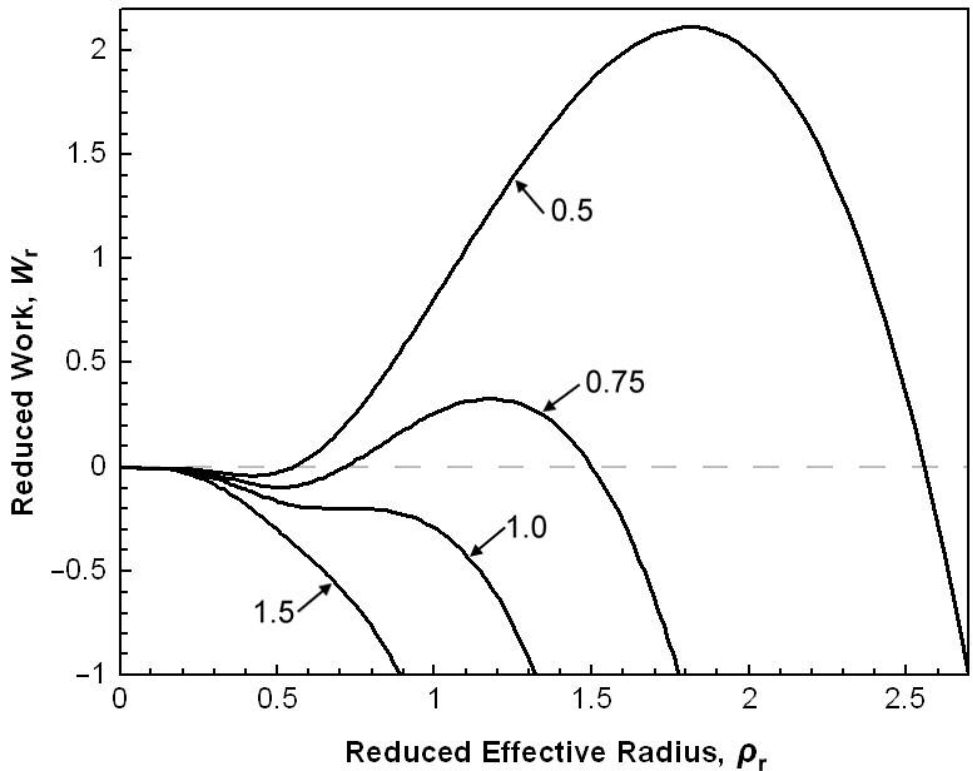


Figure 4b
282x225mm (72 x 72 DPI)

View Only

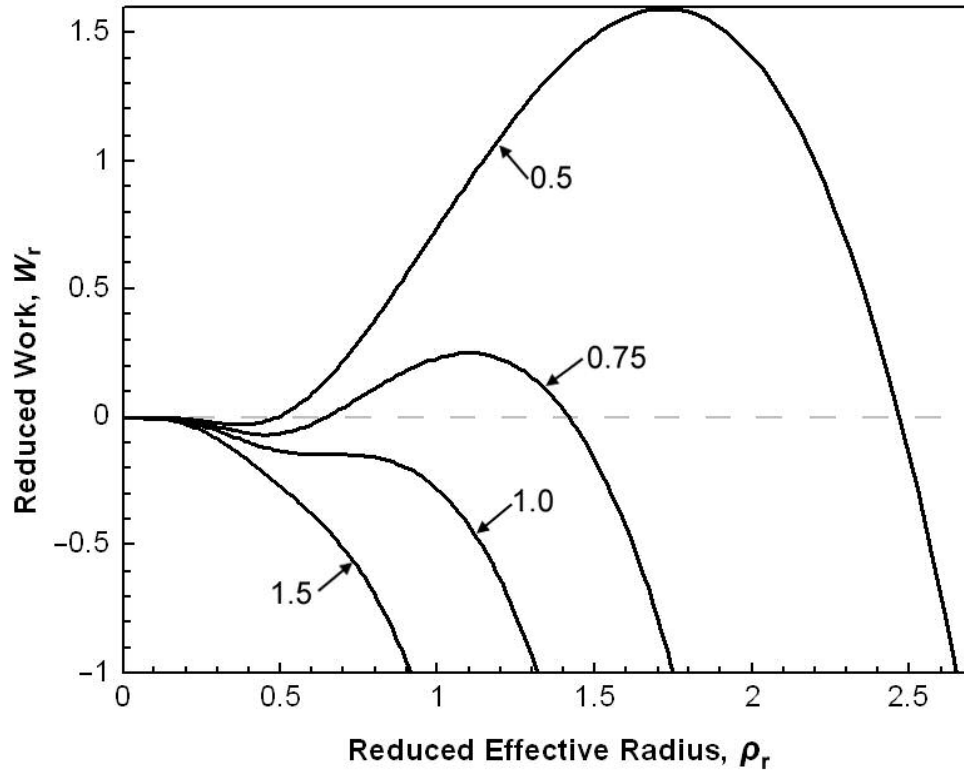


Figure 4c
282x225mm (72 x 72 DPI)

1
2
3
4
5
6
7
8
9
10
11
12
13
14
15
16
17
18
19
20
21
22
23
24
25
26
27
28
29
30
31
32
33
34
35
36
37
38
39
40
41
42
43
44
45
46
47
48
49
50
51
52
53
54
55
56
57
58
59
60

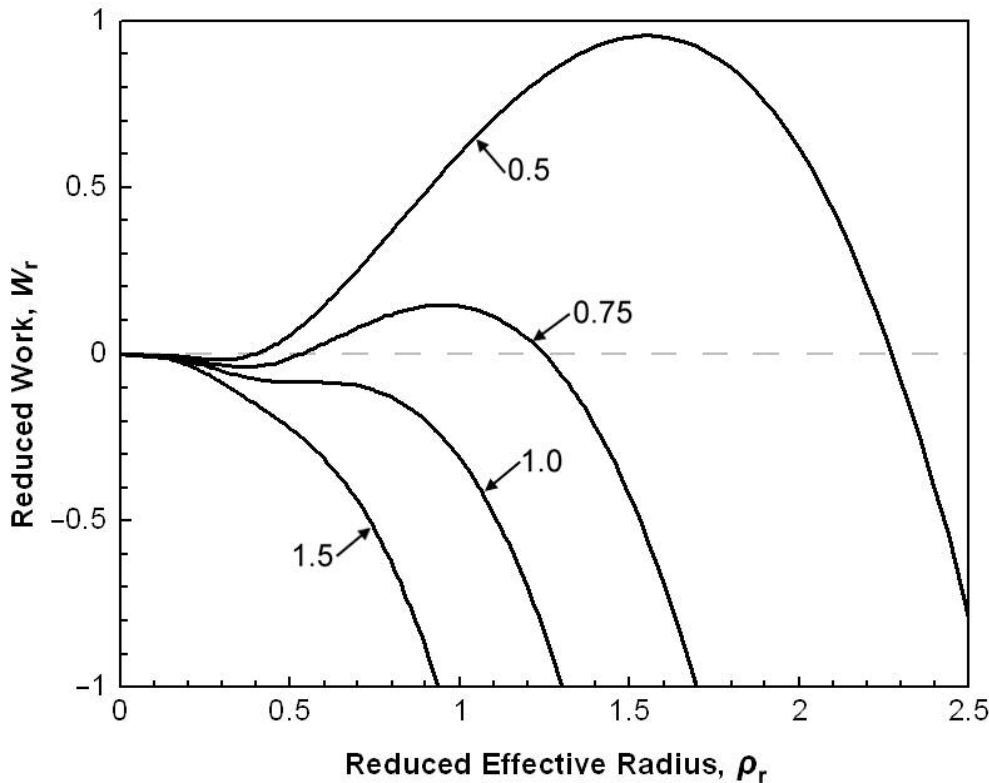


Figure 4d
282x225mm (72 x 72 DPI)

View Only

1
2
3
4
5
6
7
8
9
10
11
12
13
14
15
16
17
18
19
20
21
22
23
24
25
26
27
28
29
30
31
32
33
34
35
36
37
38
39
40
41
42
43
44
45
46
47
48
49
50
51
52
53
54
55
56
57
58
59
60

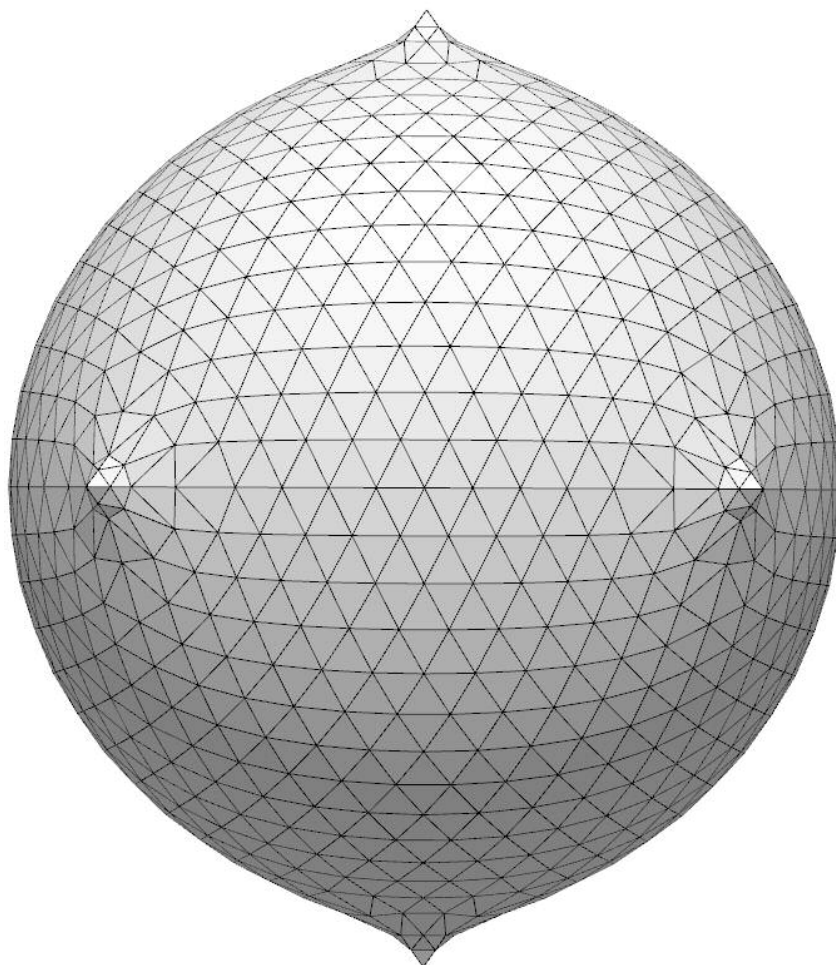


Figure 5a
282x282mm (72 x 72 DPI)



1
2
3
4
5
6
7
8
9
10
11
12
13
14
15
16
17
18
19
20
21
22
23
24
25
26
27
28
29
30
31
32
33
34
35
36
37
38
39
40
41
42
43
44
45
46
47
48
49
50
51
52
53
54
55
56
57
58
59
60

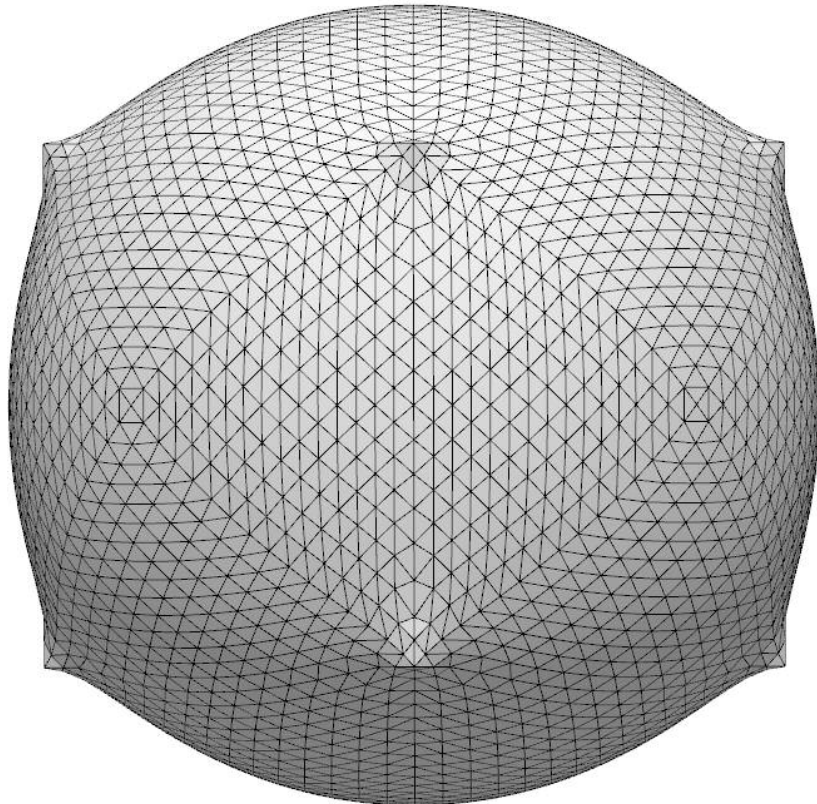


Figure 5b
282x282mm (72 x 72 DPI)



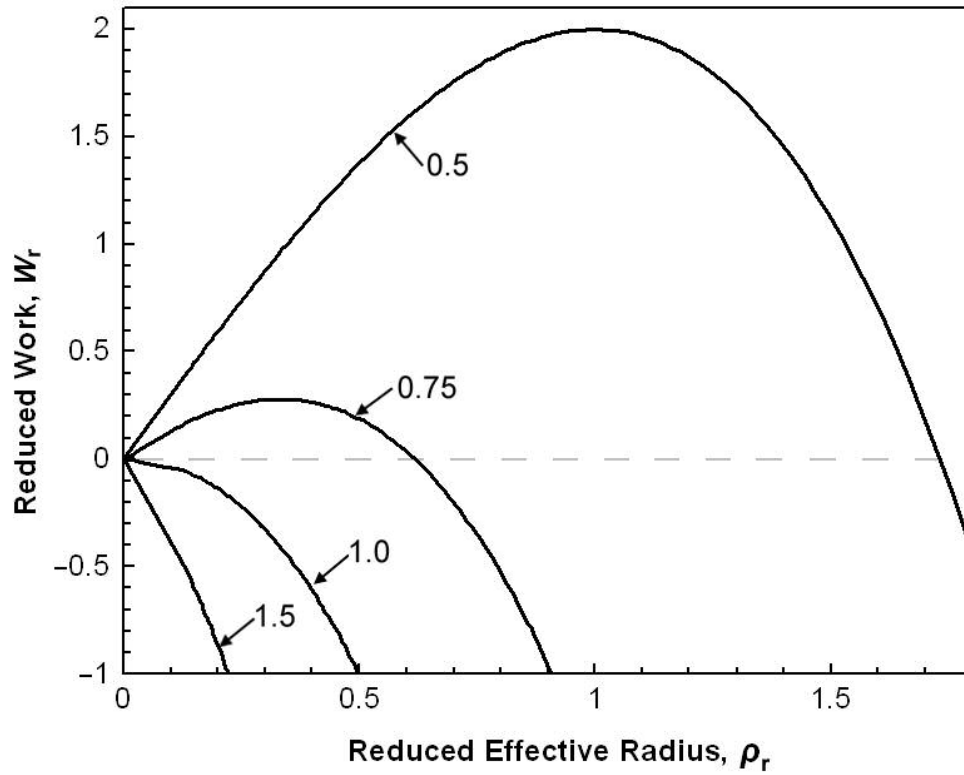


Figure 6a
282x225mm (72 x 72 DPI)

1
2
3
4
5
6
7
8
9
10
11
12
13
14
15
16
17
18
19
20
21
22
23
24
25
26
27
28
29
30
31
32
33
34
35
36
37
38
39
40
41
42
43
44
45
46
47
48
49
50
51
52
53
54
55
56
57
58
59
60

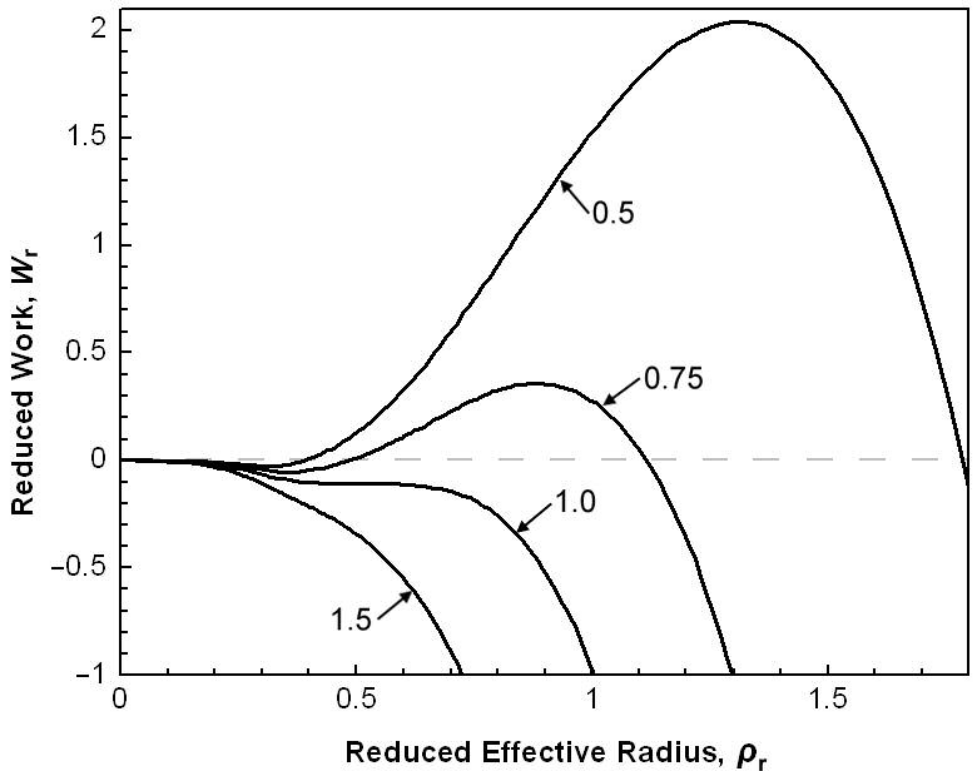


Figure 6b
282x225mm (72 x 72 DPI)

View Only

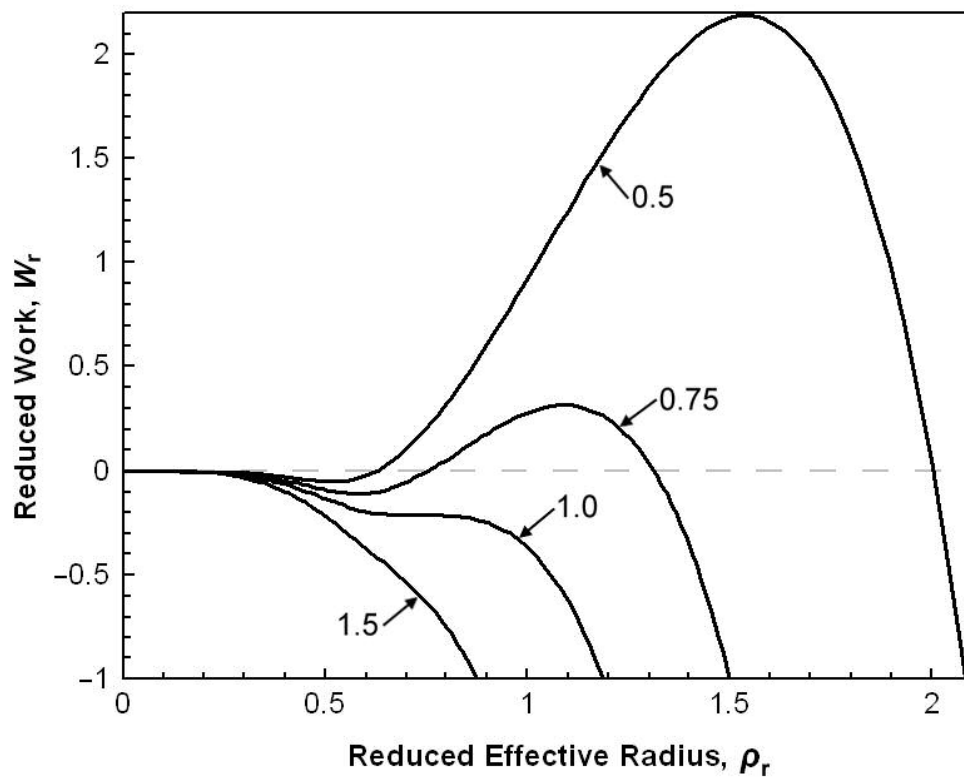


Figure 6c
282x225mm (72 x 72 DPI)

1
2
3
4
5
6
7
8
9
10
11
12
13
14
15
16
17
18
19
20
21
22
23
24
25
26
27
28
29
30
31
32
33
34
35
36
37
38
39
40
41
42
43
44
45
46
47
48
49
50
51
52
53
54
55
56
57
58
59
60

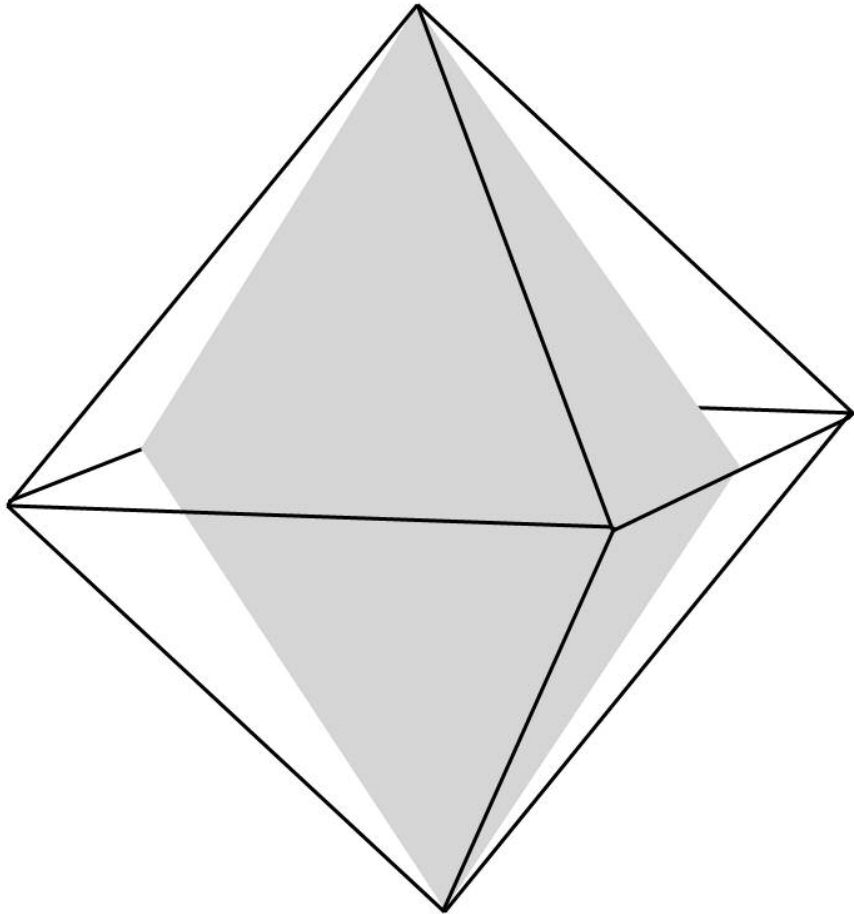


Figure 7a

only

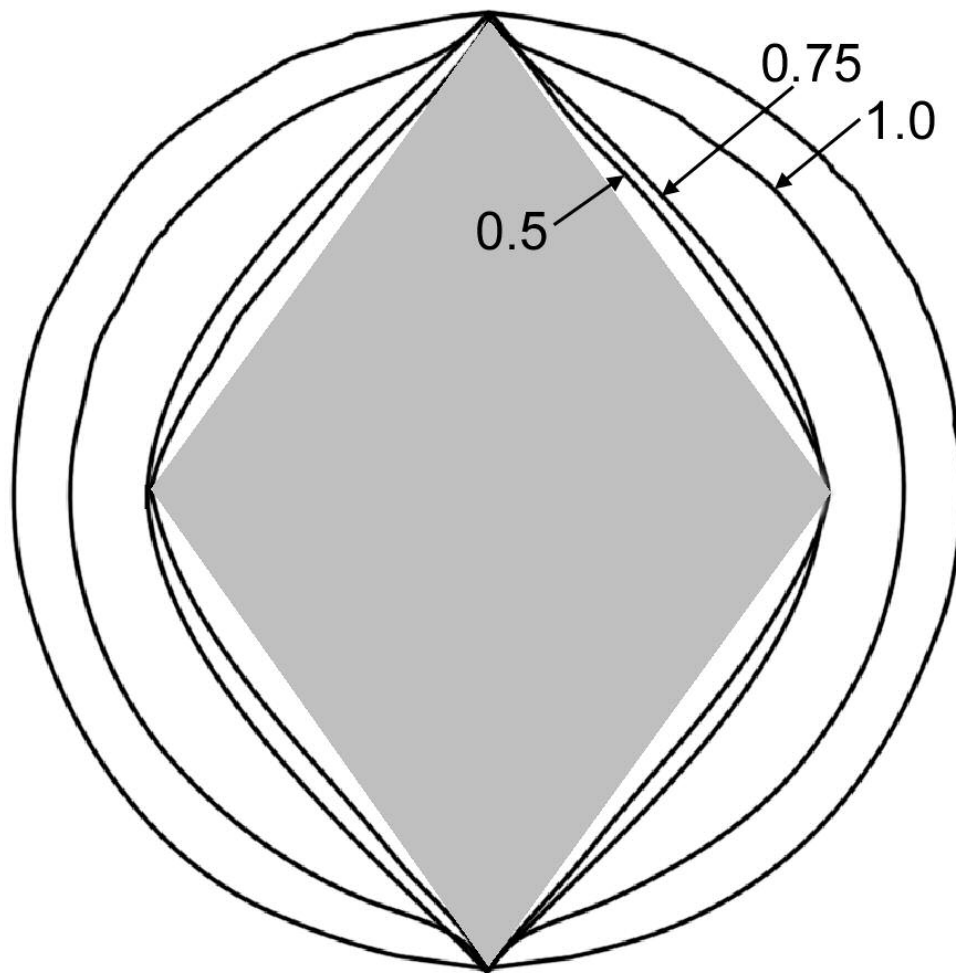


Figure 7b

only

1
2
3
4
5
6
7
8
9
10
11
12
13
14
15
16
17
18
19
20
21
22
23
24
25
26
27
28
29
30
31
32
33
34
35
36
37
38
39
40
41
42
43
44
45
46
47
48
49
50
51
52
53
54
55
56
57
58
59
60

1
2
3
4
5
6
7
8
9
10
11
12
13
14
15
16
17
18
19
20
21
22
23
24
25
26
27
28
29
30
31
32
33
34
35
36
37
38
39
40
41
42
43
44
45
46
47
48
49
50
51
52
53
54
55
56
57
58
59
60

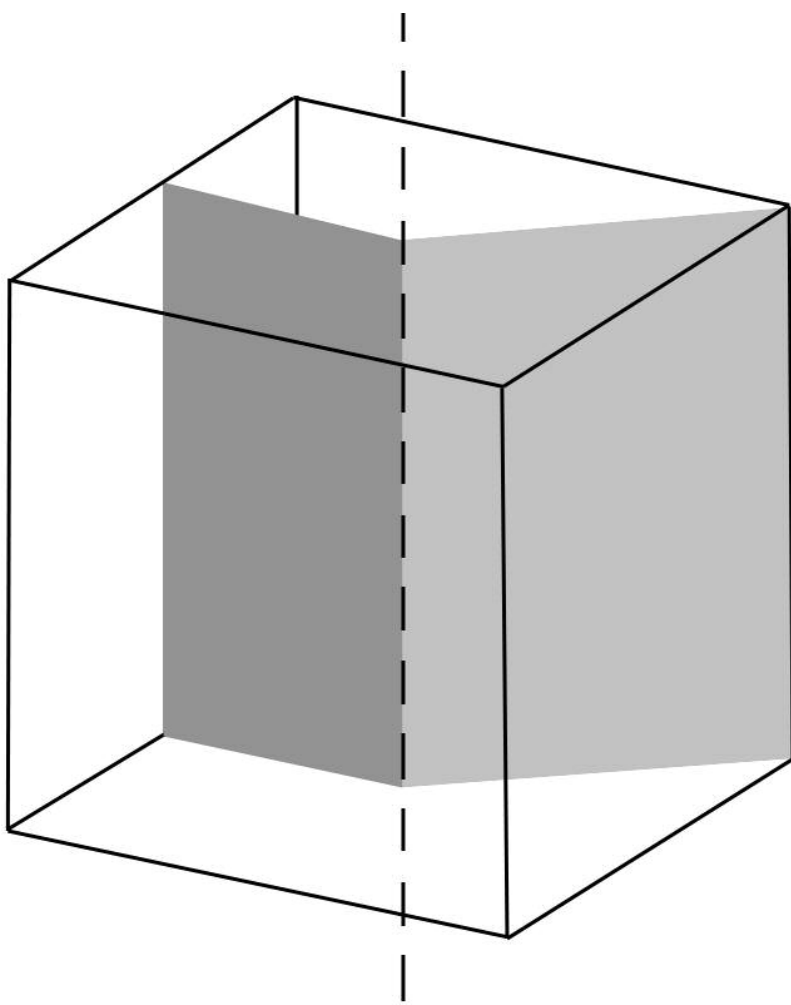


Figure 8a
282x282mm (72 x 72 DPI)



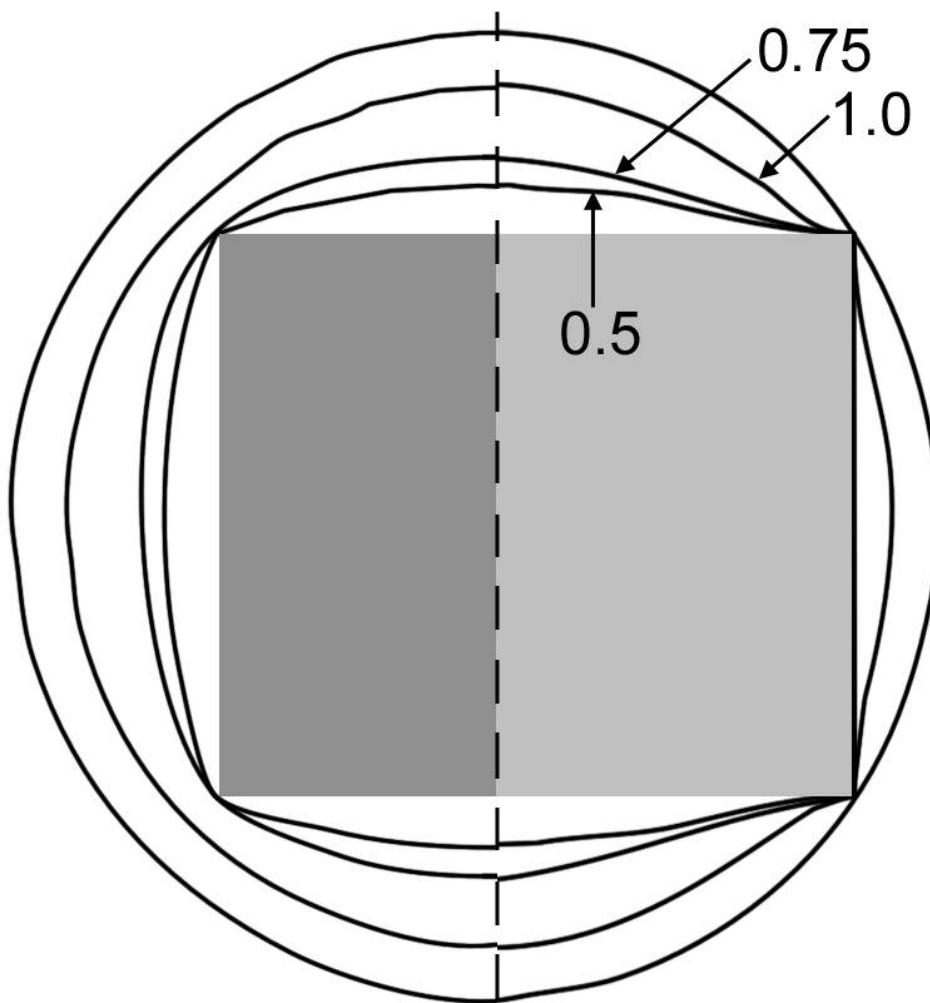


Figure 8b
282x282mm (72 x 72 DPI)



1
2
3
4
5
6
7
8
9
10
11
12
13
14
15
16
17
18
19
20
21
22
23
24
25
26
27
28
29
30
31
32
33
34
35
36
37
38
39
40
41
42
43
44
45
46
47
48
49
50
51
52
53
54
55
56
57
58
59
60

Table 1. For polygonal and polyhedral substrates, the values of β (to which the critical supercooling for the onset of free growth is proportional) have been calculated using *Surface Evolver*. For the 2D substrates, the relative areas for a given inscribing radius and the relative critical supercoolings for a given area are also given.

substrate shape	value of β in equation (10)	$\left(\frac{A(\text{polygon})}{A(\text{circle})}\right)_{\text{equal } R}$	$\left(\frac{\Delta T_{\text{fg}}(\text{polygon})}{\Delta T_{\text{fg}}(\text{circle})}\right)_{\text{equal area}}$
circle	1	1	1
hexagon	1.103 ± 0.006	0.827	1.003 ± 0.005
square	1.270 ± 0.012	0.637	1.013 ± 0.010
equilateral triangle	1.630 ± 0.036	0.413	1.048 ± 0.023
sphere	1		
cube	1.039 ± 0.004		
octahedron	1.094 ± 0.006		